J Nanostruct 10(1): 128-139, Winter 2020

RESEARCH PAPER

Electroanalytical Sensing of Asulam Based on Nanocomposite Modified Glassy Carbon Electrode

Mahmoud Roushani*, Farzaneh Mohammadi and Akram Valipour

Department of Chemistry, Ilam University, Ilam, Iran

ARTICLE INFO

Article History:
Received 09 October 2019
Accepted 22 November 2019
Published 01 January 2020

Keywords:
Asulam
Copper nanoparticles
Electrocatalytic oxidation
Ionic liquid
Multi-walled carbon nanotube

ABSTRACT

In this study a facile approach to employ Copper nanoparticle (CuNPs) and multi-walled carbon nanotubes (MWCNT) as the nanomaterial for selective detection of asulam have been investigated. This work reports the electrocatalytic oxidation of asulam on glassy carbon electrodes (GCE) modified with multi-walled carbon nanotubes (MWCNT), ionic liquids (IL), chitosan (Chit) and copper nanoparticles (CuNPs).Using the proposed nanocomposite provides a specific platform with increased surface. The surface morphology of this modified electrode was characterized by field-emission scanning electron microscopy (FE-SEM) and energy dispersive X-ray spectrometer (EDX) techniques. The electrochemical behaviors of the fabricated sensor were investigated by cyclic voltammetry (CV) and chronoamperometry modes. Under optimal conditions, the amperometric study exhibits two linear ranges of 1–11 and 11–200 μmol L^{-1} with a detection limit (LOD) of 0.33 nmol L^{-1} (at an S/N of 3) and sensitivity of 1.9 nA μmol L^{-1} for Asulam determination. This novel sensor was used to analyze the real sample. The sensor provides a convenient, low-cost and simple method for Asulam detection and proposes new horizons for quantitative detection of Asulam.

How to cite this article
Roushani M, Mohammadi F, Valipour A. Electroanalytical Sensing of Asulam Based on Nanocomposite Modified Glassy Carbon Electrode. J Nanostruct, 2020; 10(1): 128-139. DOI: 10.22052/JNS.2020.01.014

INTRODUCTION

Asulam [Methyle (4-aminobenzenesulfonyle)] carbamate is categorized into carbamate herbicide, applicable as both pre- and post-emergence herbicide absorbed by plants and then interferes with cell division and is widely used to control the growth of weeds. Its molecular structure has been illustrated in (Fig. 1). Asulam dissolves very rarely in water but their sodium salts (the commercial form) have a high solubility in water [1].

Several studies for detection of Asulam such as chemiluminescence [2-4], fluorimetric [5-7], derivatization-based dispersive liquid-liquid microextraction (DLLME) methods for spectrophotometric ultratrace determination of asulam and sulfide [8], mass spectrometry coupled to HPLC [9,10], mass spectrometry and gas chromatography [11], thin layer chromatography [12,13], HPLC [14-19] and solide phase extraction [20,21] have been developed, but a few of them have been published in electrochemistry for Asulam determination [22-25]. To the best of our knowledge, Delerue-Matos et al. investigated the use of glassy carbon electrode for the electrochemical oxidation of asulam [22], Chicharro and et al. have studied glassy carbon electrode coupled to a capillary electrophoresis instrument [23], Siswana et al. reported the use of cobalt(II) phthalocyanine modified MWCNTs [24] and nickel(II) phthalocyanine-multiwall carbon nanotubes (MWCNTs) [25] for the determination of asulam.

* *Corresponding Author Email: mahmoudroushani@yahoo.com*
m.roushani@ilam.ac.ir

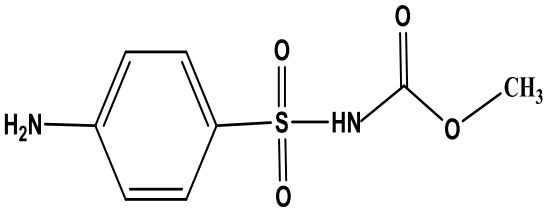

Fig. 1. Molecular structure of asulam.

Compared with other method, electrochemical sensing has exhibited several advantages including simplicity of instrument, low cost, feasibility of miniaturization and subsequent portability [26]. In the development of electrochemical sensing strategies, the signal amplification, sensitivity and stability are key factors in the improving of sensors performance. The signal amplification in the electrochemical sensors can be achieved by using nanomaterials such as graphene [27, 28], quantum dots and carbon nanotubes (CNTs). CNTs are one of the best nanomaterials used in the fabrication of electrochemical (bio) sensors. CNTs have several advantages including high chemical stability, high electrocatalytic effect, good chemical stability, high surface/volume ratio, good electrical conductivity and enhanced electron transfer that making them efficient and interest for electrodes modification [29,30]. During recent years, room temperature ionic liquids (ILs) have been widely applied in sensors and biosensors due to their unique physicochemical properties such as good conductivity, excellent biocompatibility, high viscosity and negligible vapor pressure. On the other hand, multicomponent films composed of IL offers mechanical stability and electrochemical activity [31]. Chitosan (Chit) is a linear hydrophilic polysaccharide produce by de-acetylation from chitin (a natural biopolymer obtained from fungal cell walls). It has attracted much attention due to presence of amino and hydroxyl functional groups for chemically modified electrodes (CMEs) in electrochemical analysis. Chit has attractive properties such as, good adhesion, excellent film-forming ability, good water permeability, good adhesion, susceptibility to chemical modifications, nontoxicity and biocompatibility [32]. Among the metallic nanoparticles (NPs)one of the most attractive candidates as electrode modification material (to construct chemical sensors or biosensors) is copper nanoparticles (CuNPs) due to its cheaper compared to other noble metals, good electrical conductivity, higher abundance , good catalytic and optical and thermal properties [33].

Our study is aimed fabricated an electrochemical sensor for the important herbicide Asulam using a nanocomposite of MWCNT/Chit/IL and Copper nanoparticles (CuNPs). At the first stage, nanocomposite of MWCNT/Chit/ IL was prepared and coated on the surface of glassy carbon electrode (GCE). Then GCE modified with nano-copper films by the drop casting method. The resultant electrodes exhibits excellent electrocatalytic responses towards the oxidation of Asulam with a wide linearity rang, stability, sensitivity, low detection limit and a fast amperometric response. To the best of our knowledge, the application of CuNPs/MWCNT-Chit-IL/GCE to detection of Asulam, has never been reported yet.

MATERIALS AND METHODS

Material and Reagents

Asulam was purchased from Sigma. All chemicals and reagents used in this work were of analytical grade from Merck and Sigma and used without further purification. Phosphate buffer solutions (PBS, 0.1 mol L^{-1}) with various pH values were prepared by mixing stock standard solutions of Na_2HPO_4 and NaH_2PO_4 and adjust the pH with 0.1 M H_3PO_4 or NaOH. Double-distilled water was used throughout the experiments.

Apparatus

To obtain information about The morphology of the particles of the surface modified electrodes, field- emission scanning electron microscopy (FE-SEM), energy dispersive X-ray spectroscopy (EDX) and wavelength-dispersive X-ray (WDX) spectroscopy images were recorded by a scanning electron microscope (MIRA3LMU, TESCAN). All Cyclic voltammetry (CV) and amperometric measurements studies were carried out on a µ-AUTOLAB electrochemical system type III and FRA2 board computer controlled Potentiostat/ Galvanostat (Eco-Chemie, The Switzerland) driven with NOVA software. A standard three-electrode system was used with a platinum wire as the counter electrode, Ag/AgCl (saturated with KCl) as the reference electrode and the unmodified or modified GCE served as the working electrode. pH measurement was performed by a Metrohm pH meter (model 780). All experiments were performed at room temperature.

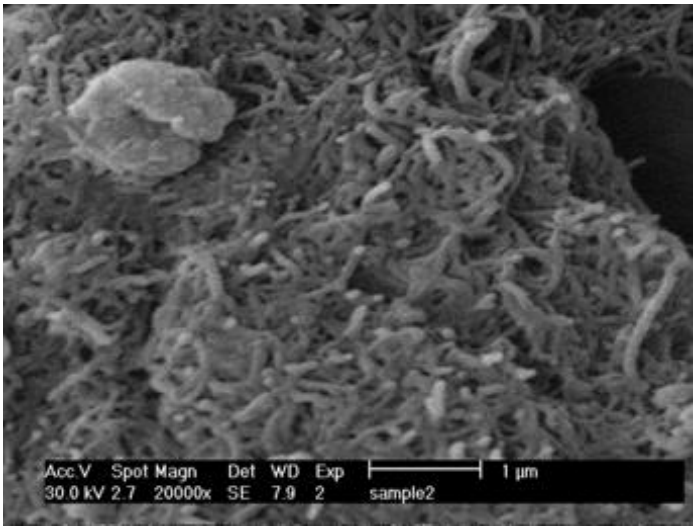

Fig. 2. Typical SEM image of MWCNTs-IL-Chit/GC electrode

Preparation of the CuNPs/ MWCNTs-IL-Chit/GCE

The CuNPs/MWCNTs-IL-Chit/GCE sensors were prepared according to following process. First, before each experiment, the Glassy carbon electrode (GCE) was polished with alumina powder on polishing paper. Successively the electrode was sonicated in 1:1 ethanol and distilled water, and then rinsed with doubly distilled water. In the next step, the cleaned GCE surface was fabricated by placing some nanocomposite paste on the electrode surface and letting it stay at room temperature (for 1h). The homogeneous black mixture of MWCNTs/IL/Chit nanocomposite was prepared by mixing of 2 mg MWCNTs, 0.2 mg Chit and 10 µL IL. This ratio obtained experimentally, and the best results were obtained when the ratio of MWCNTs to chitosan was 10:1. The amount of ionic liquid was enough to create a uniform past of Chitosan and MWCNTs. After modification of the electrode it was washed thoroughly several times with distilled water to remove adhesive materials from the electrode surface. In the next step, 10 µL of sodium acetate/acetic acid buffer solution (pH 4.5) containing 0.01 mol L^{-1} copper nitrate was pipetted onto the surface of the modified electrode and the solvent was evaporated in air and then carefully rinsed with distilled water. It was placed in a 0.5 mol L^{-1} NaCl aqueous solution at the potential range of -0.9 - 0.5 V at scan rate of 50 mVs^{-1} for 60 s. Then the electrode was immersed in a 0.1 mol L^{-1} PBS, pH 9 by cyclic scans between potentials of 0.4 and 1.3 V at a scan rate of 50 mV s^{-1} for 40 cycles until a stable voltammogram was obtained. Finally, the CuNPs/ MWCNTs-IL-Chit/ GCE sensor was ready for use after.

RESULTS AND DISCUSSION

Characterization of the CuNPs/ MWCNTs-IL-Chit/ GC Electrode

Typical SEM image of MWCNTs-IL-Chit/GC electrode is shown in Fig. 2.The FE-SEM image (Fig. 3A) clearly displayed that CuNPs were decorated on to the MWCNTs-IL-Chit/GC electrode surface. WDX analysis was used to characterize the particle distribution mapping in the electrode surface. Fig. 3B displays WDX image distribution CuNPs in GCE surface. The elemental composition of the modified electrode was confirmed by EDX analysis. The presence of Cu peak demonstrated that steady the Cu nanoparticles on the surface of the electrode, the image are shown in (Fig. 3C).

Electrochemical Characterization of the Stepwise-Modified Electrode

In this work CuNPs/ MWCNTs /IL/Chit nanocomposite was used for modification of the electrode. CV is an effective technique for probing the feature of the modified electrode surface, CV was carried out to investigate electrochemical behaviors after each assembly step. The CVs of the different modified electrodes are presented in 0.1 mmol L^{-1} phosphate buffer (pH 9) containing 0.2 mmol L^{-1} Asulam at a scan rate of 50 mV s^{-1} were observed in (Fig. 4). First, a CV of the

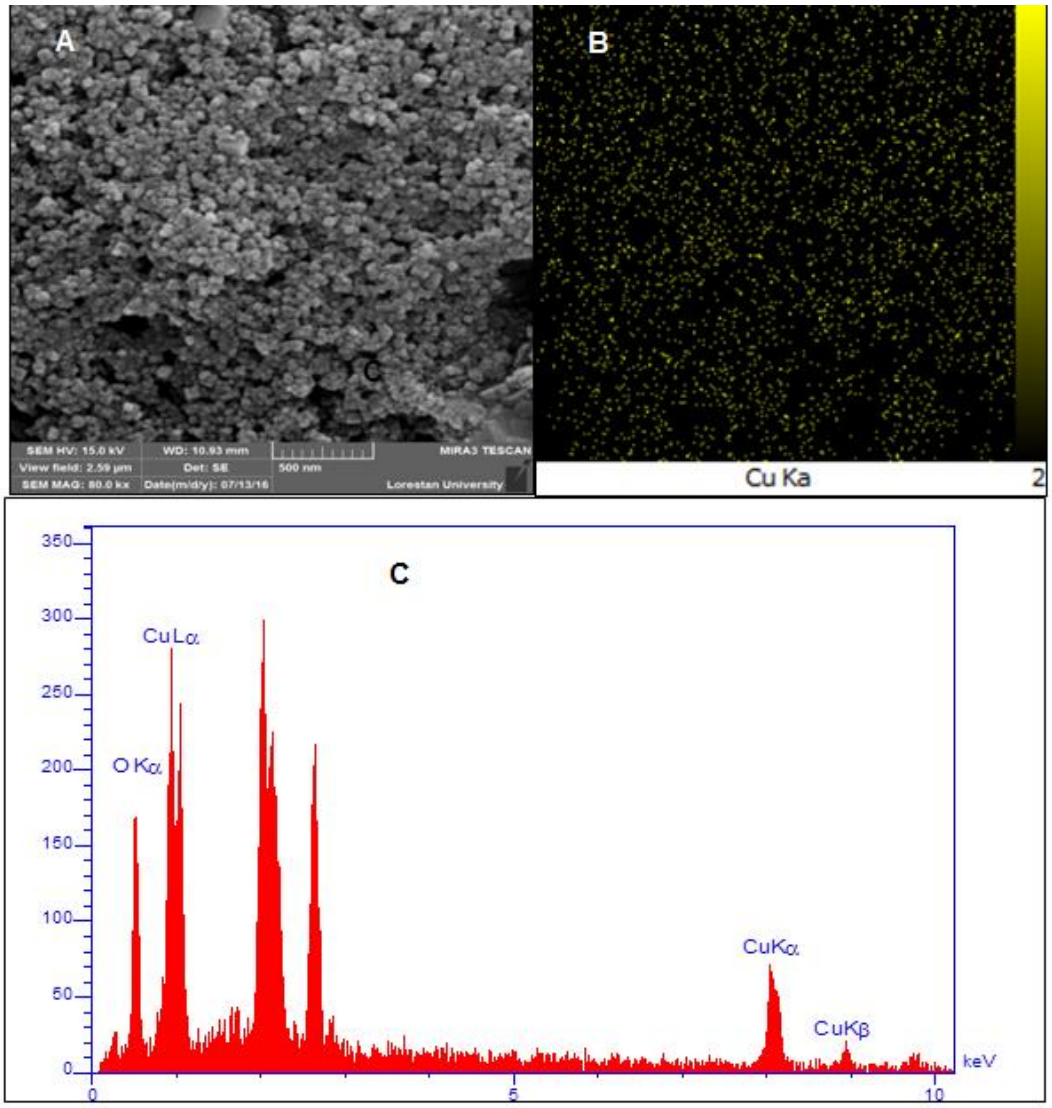

Fig. 3. Typical SEM image of CuNPs (A), WDX analysis for CuNPs (B) and Energy disperse X-ray (EDX) spectrum of the modified electrode with Cu nanoparticles (C).

bare electrode (GCE) was recorded (curve a). Secondly, the peak current was increased when the MWCNTs/IL/Chit nanocomposite was casted onto the surface of electrode which is attributed to the unique properties of nanocomposite such as excellent electric conductivity and accelerated electron transfer. The peak current further increased when the CuNPs were added onto the surface of electrode because of the attractive properties of CuNPs such as increased surface area and increased ability in electron transfer process. These results display that CuNPs/MWCNTs/IL/Chit/GC electrode has excellent improvement and suitable in facile electron transfer and increases the effective surface area for electrochemical oxidation of Asulam.

Effect of Scan Rate

For the sake of study reaction mechanism and kinetic parameters such as electron-transfer coefficient (α) and electron transfer rate constant (k°), electrochemical behavior CuNPs/ MWCNTs/ IL/Chit/GC electrode examined at various scan rates. Fig. 5A shows the CVs of the proposed sensor at different scan rates (10–100 mV s^{-1}) in phosphate buffer solution (pH 9) in the presence

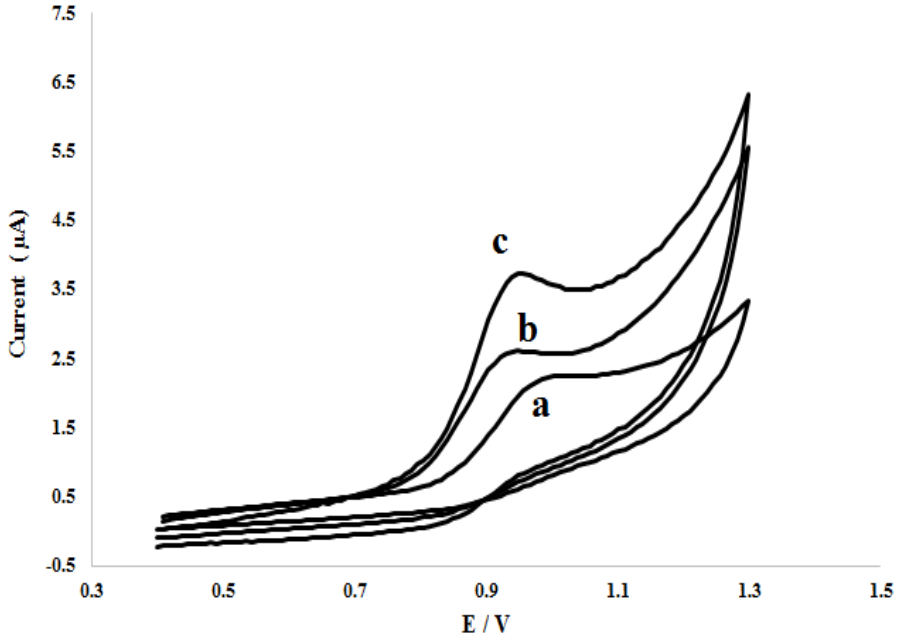

Fig. 4. CVs of bare glassy carbon electrode (a), MWCNTs-IL-Chit/GCE (b), CuNPs/ MWCNTs-IL-Chit/GCE (c) in phosphate buffer (pH 9) with the scan rate of 50 mVs^{-1} in presence of 0.2 mmol L^{-1} Asulam.

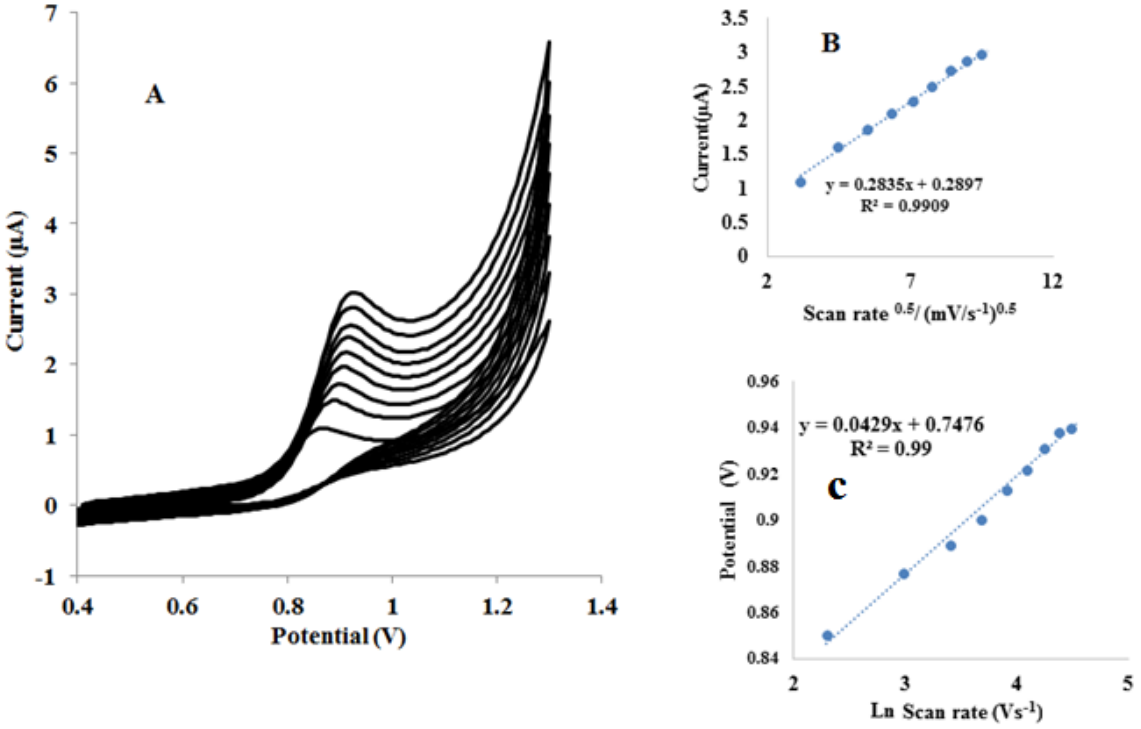

Fig. 5. (A) Cyclic voltammograms of CuNPs/ MWCNTs-IL-Chit/GC electrode in phosphate buffer (pH 9) in presence of 0.2 mmol L^{-1} Asulam at different scan rates (10–100 mV s^{-1}). (B) Plots of peak currents versus square root of scan rate. (C) Plot of peak potential (Ep) versus ln*v*.

0.2 mmol L^{-1} Asulam. From (Fig. 5B), it was obviously that the plot of anodic peak currents were linearly proportional to the square root of scan rate, its mean that electrocatalysis of Asulam is controlled by diffusion. The possible oxidation mechanism of Asulam for the CuNPs/ MWCNTs/IL/ Chit/GC electrode may be suggestion by following reactions:

Asulam (reduced form) → Asulam (oxidation form)

According to Laviron model [34] for an irreversible electrochemical reaction, by using from following equation (1):

$$E_{p=} E^{\circ} + \frac{RT}{\alpha nF} \ln\left[\frac{RTK^{\circ}}{\alpha nF}\right] + \left[\frac{RT}{\alpha nF}\right] \ln(v) \quad (1)$$

Where n is electron-transfer number; E° is formal potential; T is thermodynamic temperature; α is electron transfer coefficient; F is Faraday constant and k° is standard rate constant. The slope of the peak potential (E_p) versus Lnv (is shown in Fig.5C) produce straight line equal to *RT/αnF* that with n = 2 for electrocatalysis of Asulam reaction, a value of charge transfer coefficient (α)= 0.29 was estimated. Also the value electron transfer rate constant k° with use the intercept of the straight line of E_p vs. Ln*v* to be 5.19 s^{-1}. The value of E° was obtained from the intercept of the E_p versus v by extrapolation to the line to *v* = 0 (not shown).

Effect of pH on the Electrochemical Oxidation of Asulam

The pH of the phosphate buffer was altered in the range of 3.0 to 10.0 with the aim of evaluating the best pH value. Fig. 6A shows the CVs of the CuNPs/MWCNTs/IL/Chit/GC electrode in phosphate buffer (0.1 mol L^{-1}) containing 0.2 mmol L^{-1} Asulam at scan rate 50 mV s^{-1}. It clearly obvious with the increase of pH, peak potential has shifted to less positive potentials values. The curves showed that pH=9 due to higher current peak and better peak potential was selected as optimum pH value. As can be seen in (Fig. 6B), the plot of peak potential versus the pH (3- 10) shows an excellent linear direct relationship with a slope of ~28 mV/pH. This slope is near the Nernst equation 30 mV/pH for a two-electron reaction. However, reported in elsewhere that two- electron involves for electrocatalysis oxidation of Asulam process.

Amperometric Detection of Asulam at CuNPs/ MWCNTs/IL/Chit/ GC Electrode

Chronoamperometic technique can be employed for the estimate of the catalytic rate Constant. Fig. 7 shows the choronoamperograms of modified electrode at fixed potential of 0.9 V

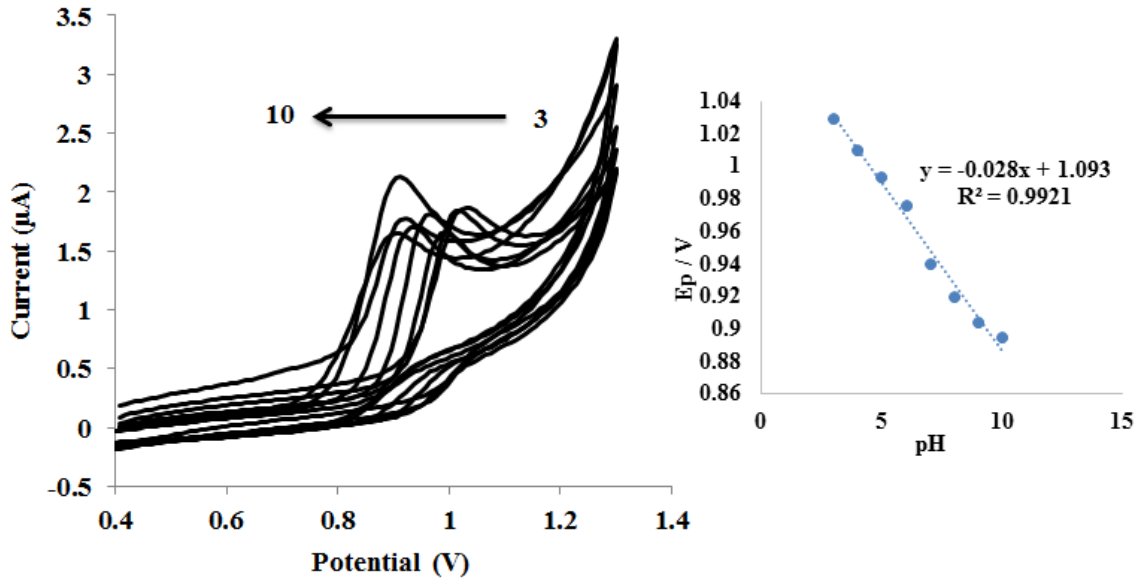

Fig. 6. (A) Cyclic voltammetric response of a CuNPs/ MWCNTs-IL-Chit/GC electrode in presence of 0.2 mmol L^{-1} asulam solutions at scan rate 50 mV s^{-1} of varying pH (pH 3–10 from right to left). (B) plot of *E*p vs. pH.

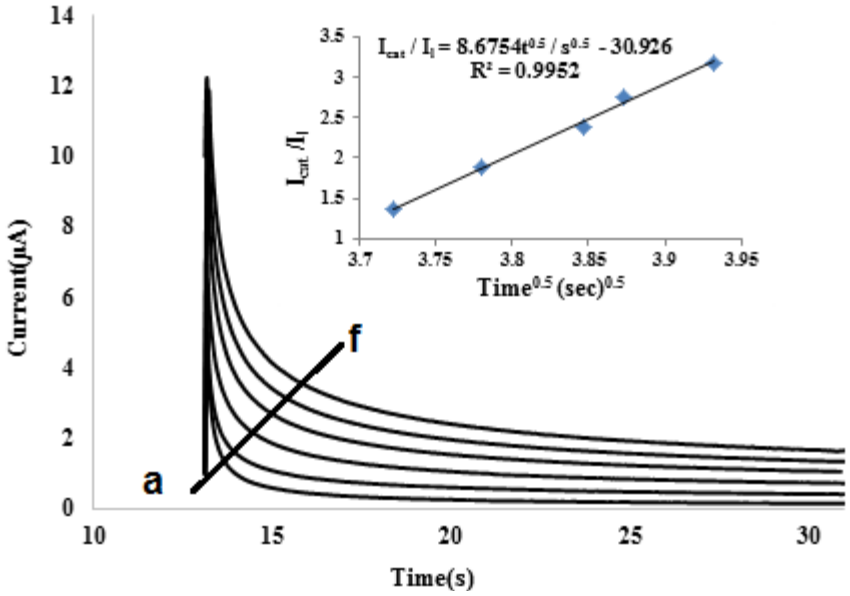

Fig. 7. Amperometric response of CuNPs/MWCNTs-IL-Chit/GC electrode in pH=9 solution containing (a) 0, (b) 0.1, (c) 0.2, (d) 0.3, (e) 0.4 (f) 0.5 mmol L^{-1} Asulam. Inset: Plot of I_{cat}/I_L *vs.* time$^{1/2}$ for average concentration of Asulam.

over 30 s in the different concentration of Asulam (0- 0.5 mmol L^{-1}). The catalytic rate constant is calculated According to the approach described in the literature [35].

$$I_{cat}/I_L = \pi^{1/2}(K_{cat}\, C_0 t)^{1/2} \quad (2)$$

I_{cat} and I_L were the oxidation currents in the presence and the absence of Asulam, respectively. K_{cat} is the catalytic rate constant ($M^{-1}s^{-1}$); C_0 is catalyst concentration (mol L^{-1}) and t is the time elapsed (s). The catalytic rate constant (K_{cat}) can be calculated from the slope of I_{cat}/I_L versus $t^{1/2}$ (inset of Fig. 7) and Eq. (2) for an average concentration of Asulam. The k_{cat} of the Asulam was estimated 5.08×10^2 M^{-1} s^{-1}.

Amperometry under stirred technique for evaluation of lower concentration of Asulam due to higher sensitivity and lower detection limit was achieved successfully. The amperometric curves response of CuNPs/ MWCNTs/IL/Chit/GC electrode at a fixed potential of 0.9 V with rotation speed 1500 rpm for different concentration 30, 5 and 1 μM of Asulam are presented in Fig. 8A, B and C, respectively. The calibration graphs for the each concentration are illustrated in the inset of the figures. This sensor displays two linear ranges from 1- 11 and 11- 200 μmol L^{-1} for oxidation of Asulam.

The detection limit (signal to noise ratio of 3) and sensitivity were obtained 0.33 nmol L^{-1} and 19 nA μM^{-1}, respectively. The result of the above experiments shows that the proposed method has more sensitivity and lower detection limit comparable with previous reports [22-25].

Fig. 9 Show cyclic voltammograms desired sensor to determine various concentrations of asulam (0.2- 3.4 mmol L^{-1}), in buffer solution (pH 9) at the scan rate of 50 mV s^{-1}. The peak current (Ip) intensity reasonably increases with increase concentration of Asulam. The inset of Fig. 8 illustrate that two linear regression equations exist for the concentration range of 0.2–3.4 mmol L^{-1}. The first range consist of concentrations between 0.2- 1.8 mmol L^{-1} with the calibration equation: y= 8.7583x + 2.2828 and a correlation coefficient R^2 = 0.9921 and the second range is consist of concentrations 1.8- 3.4 mmol $L^{-1}$with the calibration equation: y = 2.3625X + 14.34 and a correlation coefficient R^2 = 0.9952.

So far a few of electrochemical sensors have been constructed to detect of Asulam that are listed in Table 1. Therefore, it is felt that more sensors are needed to detection of Asulam. The performance of the designed sensor was superior to that of the other electrochemical sensors reported in the related literature. Furthermore, the simple fabrication process and the use of cost-

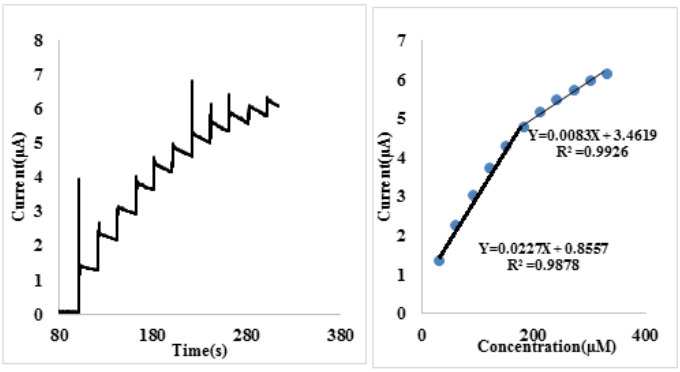

A

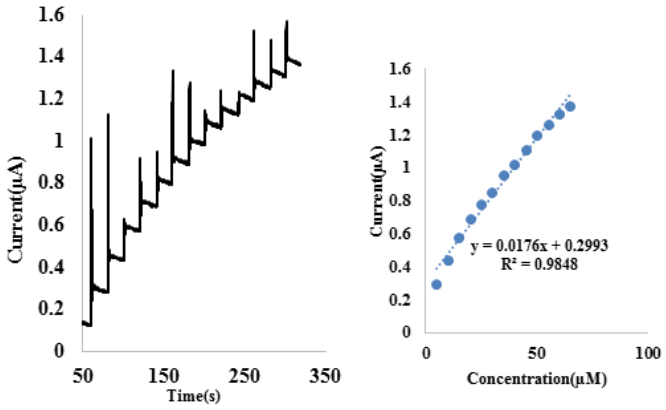

B

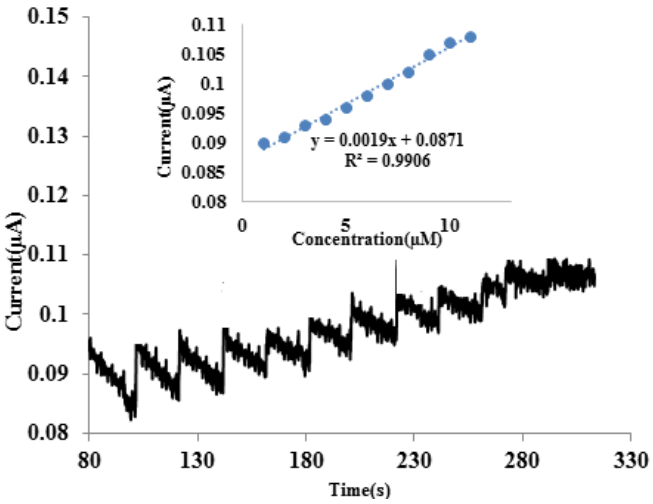

C

Fig. 8. (A) Amperometric response of CuNPs/ MWCNTs-IL-Chit/GC electrode to the additions 30 µmol L^{-1}; (B) 5 µmol L^{-1}; (C) 1 µmol L^{-1} of Asulam in phosphate buffer (pH 9) at an applied potential of 0.9 V at rotation speed is 1500 rpm . Insets: corresponding calibration curves based on the amperogram.

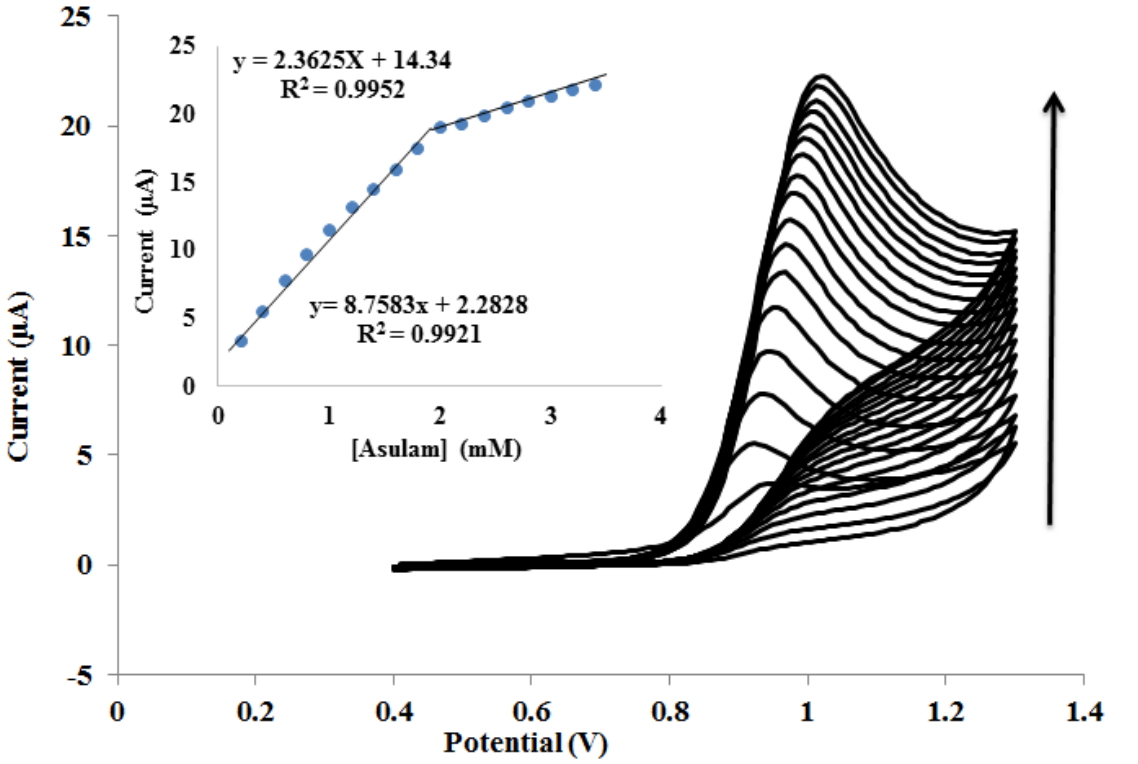

Fig. 9. CVs response of CuNPs/ MWCNTs-IL-Chit/GC sensor with increasing concentrations of asulam (from down to up: 0.2, 0.4, 0.6, 0.8, 1, 1.2, 1.4, 1.6, 1.8, 2, 2.2, 2.4, 2.6, 2.8, 3, 3.2, 3.4 mmol L^{-1}), in buffer solution ((pH 9) at the scan rate of 50 mV s^{-1}. Inset shows the calibration curve of the oxidation peak current versus the concentrations of Asulam.

effective and biocompatible compounds are major advantages in comparison to different sensors for detection of Asulam. The low detection limit and wide linear response to Asulam for proposed sensor is satisfactory. The sensitive amperometric detection performance was attributed to (1) High surface to volume ratio and electronic structure of MWCNT (2) large surface area of CuNPs. Also, this modified GCE exhibits stability, simple preparation, and inexpensive material.

Selectivity and Interference Study

The selectivity and anti-interference capability of CuNPs/MWCNTs–IL-Chit/GCE were assessed by amperometry in the presence of ascorbic acid (AA), acetaminophen (AC) and glucose for the detection of Asulam. Fig. 10 presents the amperometric responses at CuNPs/MWCNTs-IL-Chit/GCE for the successive addition of 30 µmol L^{-1} of Asulam and 3 mmol L^{-1} of each interfering substances. As shown, these compounds did not interfere with Asulam detection, indicating that the proposed sensor completely prevented the diffusion of interfering species.

Stability and Reproducibility of the Sensor

The stability of the sensor is a key factor in the practical application. As shown in Fig. 11 the amperometric response of 0.2 mmol L^{-1} Asulam was recorded over 2000 s periods. The response remained stable throughout the experiment, indicating that the sensor imparted higher stability for amperometric measurements of Asulam.

Inter-electrode and intra-electrode and coefficients of variation were used in order to investigate the reproducibility. The relative standard deviation (RSD) of reproducibility was 2.4% for 5 times measuring Asulam with the different sensors (Inter-electrode). Also for five times the reproducibility of the sensor was estimated by determining Asulam with one sensor (Intra-electrode) and RSD was calculated 3.6%.

Table 1. Comparison of different method for detection of Asulam.

Materials	Method	LR [a] (µmol.L^{-1})	LOD [b]	Ref.
NiPcNP[c]/MWCNT-BPPGE[d]	CV[e]	91–412	0.285 µmol.L^{-1}	[25]
CoTAPc[f]–MWCNT–BPPGE	SWV[g]	4.5–20	1.15 µmol.L^{-1}	[24]
CuNPs/ MWCNTs -IL-Chit	Amperometric	1–11 and 11–200	0.33 nmol.L^{-1}	This work

[a] linear rang; [b] Limit of detection; [c] Nanostructured nickel (II) phthalocyanine; [d] Basal plane pyrolytic electrode; [e] Cyclic Voltammetry; [f] Cobalt tetraaminophthalocyanine; [g] Squre wave voltammetry

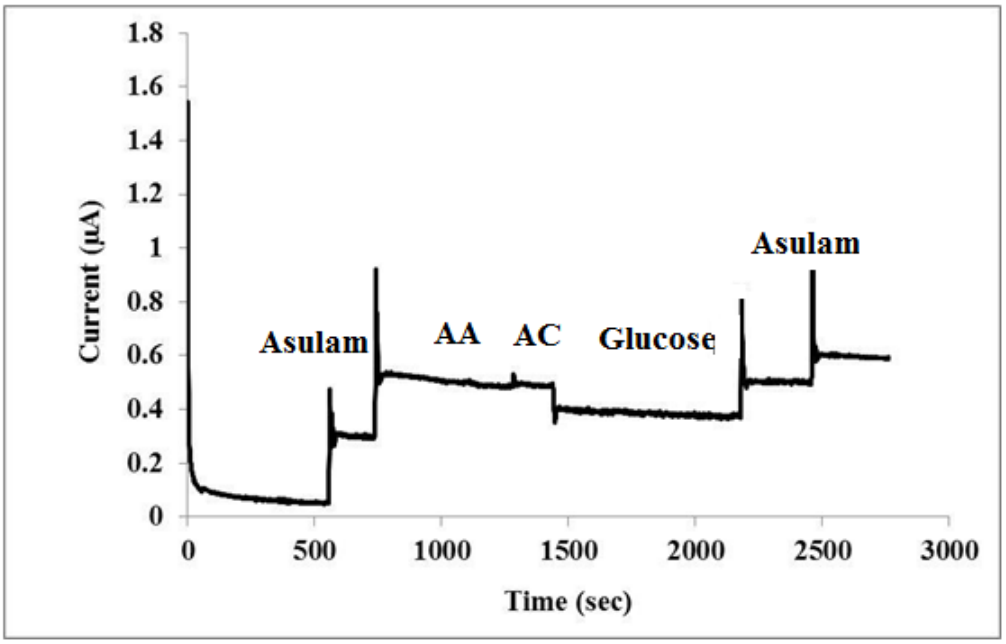

Fig. 10. Amperometric i–t response at CuNPs/MWCNTs–IL-Chit/GCE for the successive additions of 30 µmol L^{-1} Asulam, 3 mmol L^{-1} ascorbic acid (AA), 3 mmol L^{-1} acetaminophen (AC) and 3.0 mmol L^{-1} glucose

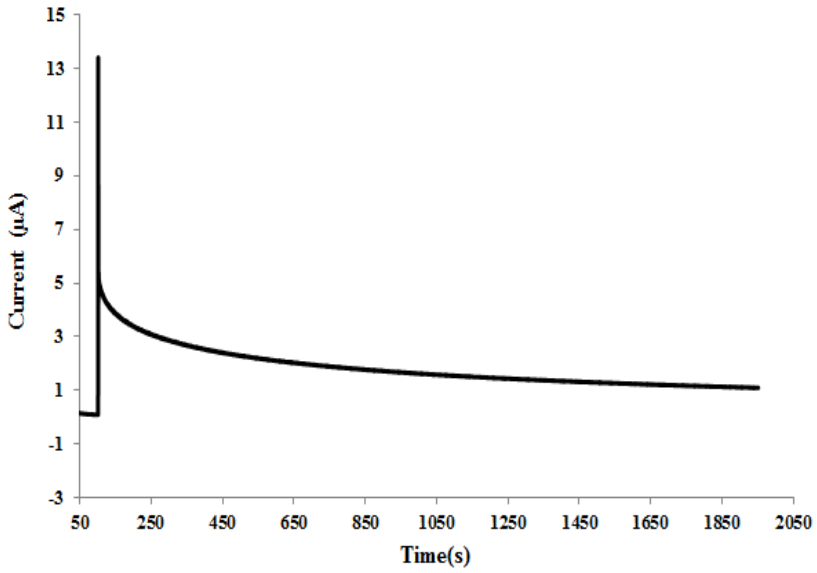

Fig. 11. Recorded chronoamperogram for 0.2 mmol L^{-1} Asulam during over 2000 s periods.

Table 2. Asulam detection in water samples with developed sensor (N=3).

sample	Real value(μM)	Found(μM)	Recovery (%) N=3
1	20	21.05±0.02	105.25
2	40	38.94±0.05	97.35
3	60	62.02±0.01	103.36

Determination of Asulam in Real Samples

Three water samples were used as real samples to test the validity of our proposed method in the real sample analysis. The concentration of Asulam was measured in an artificially prepared specimen, by adding known amounts of Asulam to samples. The standard addition method was used for determination of Asulam in this specimen. The results for the determination of Asulam in real samples are summarized in Table 2. The results of the recovery ranged from 97 to 105% for the determination of Asulam in samples. The detected result revealed that this sensor could be used for the measurement of Asulam in water sample test.

CONCLUSION

One of the important problems in our world is population. The use of high doses toxicants agriculture creates destructive effects on human and animals healthy thus its need techniques such as novel electrochemical methods with low cost, simple preparation procedure, speed and high sensitive toward the determination of toxicants. In this work a new electrochemical sensor was prepared, which avoids using expensive materials, to make the detection of Asulam (as a toxicant) cheaper, faster and simpler. The reported method provides a promising MWCNTS/IL/Chit/CuNPs nanocomposite for different analytes. CuNPs was successfully synthesized and used to modify the working electrode. CuNPs have been immobilized onto the amine groups of chitosan and provide a good substratum for reactions on the surface of electrode. This sensor exhibits good electroanalytical activities such as excellent sensitivity, high efficiency and lower detection limit for Asulam analysis.

ACKNOWLEDGMENT

This study has been supported by the Ilam University.

CONFLICT OF INTEREST

The authors declare that there is no conflict of interests regarding the publication of this manuscript.

REFERENCES

1. Li T-L, Lee W-Ch, Chang Pi-Ch, Chou Sh-Sh. High performance chromatographic determination of asulam residue in agricultural products. J Food Drug Anal. 2001;9(1):40-44.
2. Sánchez FG, Díaz AN, Bracho V, Aguilar A, Algarra M. Automated determination of asulam by enhanced chemiluminescence using luminol/peroxidase system. Luminescence. 2009:n/a-n/a.
3. García Sánchez F, Navas Díaz A, Delgado Téllez C, Algarra M. Determination of asulam by fast stopped-flow chemiluminescence inhibition of luminol/peroxidase. Talanta. 2008;77(1):294-7.
4. Chivulescu A, Catalá-Icardo M, García Mateo JV, Martínez Calatayud J. New flow-multicommutation method for the photo-chemiluminometric determination of the carbamate pesticide asulam. Analytica Chimica Acta. 2004;519(1):113-20.
5. Sánchez FG, Díaz AN, Pareja AG, Bracho V. Liquid Chromatographic Determination of Asulam and Amitrole with Pre-Column Derivatization. Journal of Liquid Chromatography & Related Technologies. 1997;20(4):603-15.
6. Uacute, Bov, Aacute, I., Khenlami Assandas A, Catal, et al. Fluorescence Determination of the Pesticide Asulam by Flow Injection Analysis. Analytical Sciences. 2006;22(1):21-4.
7. Sánchez FG, Díaz AN, Pareja AG. Ion-pair reversed-phase liquid chromatography with fluorimetric detection of pesticides. Journal of Chromatography A. 1994;676(2):347-54.
8. Eskandari H, Shahbazi-Raz M. Ionic liquid based microextraction combined with derivatization for efficient enrichment/determination of asulam and sulfide. TURKISH JOURNAL OF CHEMISTRY. 2016;40:1019-33.
9. Moreno-González D, Gámiz-Gracia L, García-Campaña AM, Bosque-Sendra JM. Use of dispersive liquid–liquid microextraction for the determination of carbamates in juice samples by sweeping-micellar electrokinetic chromatography. Analytical and Bioanalytical Chemistry. 2011;400(5):1329-38.
10. Hu J-Y, Aizawa T, Magara Y. Analysis of pesticides in water with liquid chromatography/atmospheric pressure chemical ionization mass spectrometry. Water Research. 1999;33(2):417-25.
11. Tsuji H, Henmi N, Kaneda Y. Gas Chromatographic and Mass

Spectrometric Determination of Asulam, Mecoprop and Trichlorfon in Water Sample. Eisei kagaku. 1995;41(4):292-9.
12. Smith AE, Milward LJ. Thin-layer chromatographic detection of the herbicide asulam in soils and the identification of sulphanilamide as a minor soil degradation product. Journal of Chromatography A. 1983;265:378-81.
13. Butz S, Stan HJ. Screening of 265 Pesticides in Water by Thin-Layer Chromatography with Automated Multiple Development. Analytical Chemistry. 1995;67(3):620-30.
14. Suzuki T, Yaguchi K, Kano I. Screening methods for asulam, oxine-copper and thiram in water by high-performance liquid chromatography after enrichment with a minicolumn. Journal of Chromatography A. 1993;643(1-2):173-9.
15. Kaniansky D, Madajová V, Hutta M, Žilková I. Analysis of asulam in soil by isotachophoresis and liquid chromatography. Journal of Chromatography A. 1984;286:395-406.
16. Gennaro MC, Abrigo C, Giacosa D, Rigotti L, Liberatori A. Separation of phenylurea pesticides by ion-interaction reversed-phase high-performance liquid chromatography Diuron determination in lagoon water. Journal of Chromatography A. 1995;718(1):81-8.
17. Uemori H, Yoshida K, Fukumoto M, Kondo K, Matsuura S. Simultaneous determination of pesticides used on golf courses in drinking and river water by cyanopropyl bonded silica phase HPLC. Bunseki kagaku. 1995;44(6):443-7.
18. Lawrence JF, Panopio LG, McLeod HA. Direct analysis of the wild oat herbicide, asulam, in wheat samples by reversed-phase liquid chromatography at selected ultraviolet wavelengths. Journal of Agricultural and Food Chemistry. 1980;28(6):1323-5.
19. Kon RT, Geissel L, Leavitt RA. An h.p.l.c. method for the quantitative determination of asulam, acetylasulam and sulphanilamide in peachesa. Food Additives & Contaminants. 1984;1(1):67-71.
20. Mol HGJ, Rooseboom A, van Dam R, Roding M, Arondeus K, Sunarto S. Modification and re-validation of the ethyl acetate-based multi-residue method for pesticides in produce. Analytical and Bioanalytical Chemistry. 2007;389(6):1715-54.
21. Kerkdijk H, Mol HGJ, van der Nagel B. Volume Overload Cleanup: An Approach for On-Line SPE-GC, GPC-GC, and GPC-SPE-GC. Analytical Chemistry. 2007;79(21):7975-83.
22. Nouws H, Delerue-Matos C, Lima J, Garrido EM, Vincke P, Maes N. Electroanalytical Study of the Pesticide Asulam. International Journal of Environmental Analytical Chemistry. 2002;82(2):69-76.
23. Chicharro M, Zapardiel A, Bermejo E, Sánchez A. Simultaneous UV and electrochemical determination of the herbicide asulam in tap water samples by micellar electrokinetic capillary chromatography. Analytica Chimica Acta. 2002;469(2):243-52.
24. Siswana MP, Ozoemena KI, Nyokong T. Electrocatalysis of asulam on cobalt phthalocyanine modified multi-walled carbon nanotubes immobilized on a basal plane pyrolytic graphite electrode. Electrochimica Acta. 2006;52(1):114-22.
25. Siswana MP, Ozoemena KI, Geraldo DA, Nyokong T. Nanostructured nickel (II) phthalocyanine—MWCNTs as viable nanocomposite platform for electrocatalytic detection of asulam pesticide at neutral pH conditions. Journal of Solid State Electrochemistry. 2009;14(8):1351-8.
26. Roushani M, Valipour A, Valipour M. Layer-by-layer assembly of gold nanoparticles and cysteamine on gold electrode for immunosensing of human chorionic gonadotropin at picogram levels. Materials Science and Engineering: C. 2016;61:344-50.
27. Roushani M, Valipour A. Using electrochemical oxidation of Rutin in modeling a novel and sensitive immunosensor based on Pt nanoparticle and graphene–ionic liquid–chitosan nanocomposite to detect human chorionic gonadotropin. Sensors and Actuators B: Chemical. 2016;222:1103-11.
28. Roushani M, Valipour A. Voltammetric immunosensor for human chorionic gonadotropin using a glassy carbon electrode modified with silver nanoparticles and a nanocomposite composed of graphene, chitosan and ionic liquid, and using riboflavin as a redox probe. Microchimica Acta. 2015;183(2):845-53.
29. Chawla S, Rawal R, Pundir CS. Fabrication of polyphenol biosensor based on laccase immobilized on copper nanoparticles/chitosan/multiwalled carbon nanotubes/polyaniline-modified gold electrode. Journal of Biotechnology. 2011;156(1):39-45.
30. Dorraji PS, Jalali F. Sensitive amperometric determination of methimazole based on the electrocatalytic effect of rutin/multi-walled carbon nanotube film. Bioelectrochemistry. 2015;101:66-74.
31. Lo N-C, Tang Y-H, Kao C-L, Sun IW, Chen P-Y. Electrochemical formation of palladium nanoparticles in a salicylate-based hydrophilic ionic liquid: The effect of additives on particle morphology and electrochemical behavior. Electrochemistry Communications. 2016;62:60-3.
32. Chien R-C, Yen M-T, Mau J-L. Antimicrobial and antitumor activities of chitosan from shiitake stipes, compared to commercial chitosan from crab shells. Carbohydrate Polymers. 2016;138:259-64.
33. Devasenathipathy R, Kohilarani K, Chen S-M, Wang S-F, Wang S-C, Chen C-K. Electrochemical preparation of biomolecule stabilized copper nanoparticles decorated reduced graphene oxide for the sensitive and selective determination of hydrogen peroxide. Electrochimica Acta. 2016;191:55-61.
34. Laviron E, Roullier L. General expression of the linear potential sweep voltammogram for a surface redox reaction with interactions between the adsorbed molecules. Journal of Electroanalytical Chemistry and Interfacial Electrochemistry. 1980;115(1):65-74.
35. Pournaghi-Azar MH, Sabzi R. Electrochemical characteristics of a cobalt pentacyanonitrosylferrate film on a modified glassy carbon electrode and its catalytic effect on the electrooxidation of hydrazine. Journal of Electroanalytical Chemistry. 2003;543(2):115-25.